Available online at www.sciencedirect.com
SCIENCE DIRECT®
Journal of Organometallic Chemistry 690 (2005) 885–894
Journal of Organometallic Chemistry
www.elsevier.com/locate/jorganchem

Syntheses and characterization of $[(\eta^6\text{-}C_6Me_6)Ru(\mu\text{-}N_3)(X)]_2$ (X = N_3 and Cl) complexes and their reactions towards mono- and bidentate ligands ☆

P. Govindaswamy [a], Patrick J. Carroll [b], Yurij A. Mozharivskyj [c], Mohan Rao Kollipara [a,*]

[a] Department of Chemistry, North-Eastern Hill University, Shillong 793 022, India
[b] Department of Chemistry, University of Pennsylvania, Philadelphia, Pennsylvania, PA 19104, USA
[c] Ames Laboratory, Iowa State University of Science and Technology, Ames, Iowa, IA 50011, USA

Received 25 August 2004; accepted 16 October 2004
Available online 21 November 2004

Abstract

The reaction of the complex $[\{(\eta^6\text{-}C_6Me_6)Ru(\mu\text{-}Cl)Cl\}_2]$ **1** with sodium azide ligand gave two new dimers of the composition $[\{(\eta^6\text{-}C_6Me_6)Ru(\mu\text{-}N_3)(N_3)\}_2]$ **2** and $[\{(\eta^6\text{-}C_6Me_6)Ru(\mu\text{-}N_3)Cl\}_2]$ **3**, depending upon the reaction conditions. Complex **3** with excess of sodium azide in ethanol yielded complex **2**. These complexes undergo substitution reactions with monodentate ligands to yield monomeric complexes of the type $[(\eta^6\text{-}C_6Me_6)Ru(X)(N_3)(L)]$ {X = N_3, Cl, L = PPh_3 (**4a**, **9a**); PMe_2Ph (**4b**, **9b**); $AsPh_3$ (**4c**, **9c**); X = N_3, L = pyrazole (Hpz) (**5a**); 3-methylpyrazole (3-Hmpz) (**5b**) and 3,5-dimethyl-pyrazole (3,5-Hdmpz) (**5c**)}. Complexes **2** and **3** also react with bidentate ligands to give bridging complexes of the type $[\{(\eta^6\text{-}C_6Me_6)Ru(N_3)(X)\}_2(\mu\text{-}L)]$ {X = N_3, Cl, L = 1,2-bis(diphenylphosphino)methane (dppm) (**6**, **10**); 1,2-bis(diphenylphosphino)ethane (dppe) (**7**, **11**); 1,2-bis(diphenylphosphino)propane (dppp) (**8**, **12**); X = Cl, L = 4,4-bipyridine (4,4′-bipy) (**13**)}. These complexes were characterized by FT-IR and FT-NMR spectroscopy as well as by analytical data.The molecular structures of the representative complexes $[\{(\eta^6\text{-}C_6Me_6)Ru(\mu\text{-}N_3)(N_3)\}_2]$ **2**, $[\{(\eta^6\text{-}C_6Me_6)Ru(\mu\text{-}N_3)Cl\}_2]$ **3**,$[(\eta^6\text{-}C_6Me_6)Ru(N_3)_2(PPh_3)]$ **4a** and $[\{(\eta^6\text{-}C_6Me_6)Ru(N_3)_2\}_2$ (μ-dppm)] **6** were established by single crystal X-ray diffraction studies.

Keywords: Hexamethylbenzene; Azide; Phosphines; Pyrazoles and ruthenium

1. Introduction

In recent years, the coordination chemistry of chelated ligands containing mixed functionalities on transition metal centers has been an extremely active area of research [1]. In particular, transition metal complexes having a coordination group which is π electron bonded (like the cyclopentadienyl ligand) have attracted attention from the viewpoints of improving and elucidating catalytic processes such as olefin polymerization [2–5]. A lot of interest has been generated in these complexes due to the synthesis of water-soluble arene ruthenium complexes which exhibit antibiotic, antiviral [6] and catalytic activities [7]. Recently, the first half-sandwich arene ruthenium(II)–enzyme complex was isolated by the reaction of η^6-*p*-cymene Ru(II) complexes with hen egg-white lysozyme [8]. We have been interested in supramolecular arene ruthenium complexes based on

☆ A part of the initial results was published as a note in J. Organomet. Chem., 689 (2004) 3108.

* Corresponding author. Tel.: +91 364 272 2620; fax: 91 364 2550076.
E-mail addresses: kmrao@nehu.ac.in, mrkollipara@yahoo.com (M.R. Kollipara).

0022-328X/$ - see front matter © 2004 Elsevier B.V. All rights reserved.
doi:10.1016/j.jorganchem.2004.10.039

quasi-octahedral geometries, since a new type of supramolecular series could be developed by introduction of these organic moieties [9]. Recently, Chang et al. [10] reported cyclopentadienyl ruthenium azide [(η^5-C_5H_5)Ru(PPh_3)$_2$(N_3)] complexes and their reactions with acetylenes yielded triazoles and tetrazoles. We have recently communicated syntheses of azide dimeric complexes of ruthenium(II) [11] along with their reactions with monodentate ligands. We have also reported reactivity studies of chloro arene ruthenium dimers [{(η^6-arene)Ru(μ-Cl)Cl}$_2$] with diphenyl-2-pyridyl-phosphine (PPh_2Py) and pyrazoles to yield neutral, cationic phosphine compounds and amidine complexes, as well as disubstituted pyrazole complexes [12]. No reports are available yet on the reactivity of these complexes with azide groups.

We here report the preparation of new azide ruthenium(II) dimers containing the hexamethylbenzene group and their reactions with a variety of mono- and bidentate ligands. We have isolated mononuclear and binuclear complexes in these reactions. Representative complexes have been characterized by single crystal X-ray study.

2. Experimental

2.1. General considerations

All chemicals used were of reagent grade. The solvents were dried and distilled before use following the standard procedures. Ruthenium trichloride trihydrate (Arora Matthey Ltd.), hexamethylbenzene (Acros Organics), PPh_3, $PPhMe_2$, $AsPh_3$, 1,2-bis-(diphenylphosphino)methane (dppm), 1,2-bis(diphenylphosphino)ethane (dppe), 1,2-bis-(diphenylphosphino)-propane (dppp) (Aldrich), sodium azide (Loba), 4,4′-bipyridine (4,4′-bipy), pyrazole (Hpz), and 3-methylpyrazole (3-Hmpz) (Merck) were used as received. The ligand 3,5-dimethylpyrazole and the precursor complex [{(η^6-C_6Me_6)Ru(μ-Cl)Cl}$_2$] **1** were prepared according to the literature procedures [12b,13]. Elemental analyses of the complexes were performed in a Perkin–Elmer-2400 CHN/O analyzer. Infrared spectra were recorded on a Perkin–Elmer 983 spectrophotometer. ^{1}H and ^{31}P {^{1}H} NMR spectra were recorded on a Bruker-ACF-300 (300 MHz) NMR spectrometer and referenced to tetramethylsilane and H_3PO_4 (85%), respectively. Coupling constants J are given in hertz (Hz).

2.2. Synthesis of [(η^6-C_6Me_6)Ru(μ-N_3)(N_3)]$_2$ (**2**)

A mixture of [(η^6-C_6Me_6)$RuCl_2$]$_2$ (100 mg, 0.149 mmol) and excess of sodium azide (60 mg, 0.897 mmol) was stirred in dry ethanol (25 ml) for 4 h whereby the orange-colored product was separated out. The compound was filtered, washed with dry ethanol and diethylether and dried under vacuum (yield 95 mg, 92%).

IR (KBr pellets, cm^{-1}): 2064s (μ-ν_{N3}), 2024s (terminal ν_{N3}). ^{1}H NMR ($CDCl_3$, δ): 2.06 (s, 36H, HMB). Elemental analysis (%) for $C_{24}H_{36}Ru_2N_{12}$: Calculated – C, 33.87; H, 5.90; N, 27.43. Found: C, 33.32; H, 6.21; N, 27.33.

2.3. Synthesis of [(η^6-C_6Me_6)Ru(μ-N_3)(Cl)]$_2$ (**3**)

A mixture of [(η^6-C_6Me_6)$RuCl_2$]$_2$ **1** (100 mg, 0.149 mmol) and twofold excess of sodium azide (18 mg, 0.288 mmol) was stirred in dry acetone (20 ml) for 10 h whereby the orange-red colored product was separated out. The compound was filtered, washed with dry ethanol and diethylether and dried under vacuum (yield 87 mg, 85%).

IR (KBr pellets, cm^{-1}): 2057s (μ-ν_{N3}). ^{1}H NMR ($CDCl_3$, δ): 2.09 (s, 36H, HMB). Elemental analysis (%) for $C_{24}H_{36}Ru_2N_6Cl_2$: Calculated – C, 42.2; H, 5.32; N, 12.32. Found: C, 42.38; H, 5.09; N, 12.44.

2.4. Synthesis of complex **2** (second method)

A mixture of complex **3** (100 mg, 0.146 mmol) and excess of sodium azide (38 mg, 0.587 mmol) was stirred in dry ethanol (20 ml) for 2 h, whereby the orange-colored product was separated out. The compound was filtered, washed with diethylether and dried under vacuum (yield 86 mg, 84%).

2.5. Synthesis of [(η^6-C_6Me_6)Ru(N_3)$_2$ (L)] {L = PPh_3 (**4a**), PMe_2Ph (**4b**) $AsPh_3$ (**4c**)}

A mixture of complex **2** (60 mg, 0.086 mmol) and ligand **L** (0.260 mmol) was stirred in dry acetone (10 ml) for 12 h, whereby the orange-colored product was separated out. The compound was filtered, washed with diethylether and dried under vacuum.

2.5.1. Complex **4a**

Yield 45 mg (43%). IR (KBr pellets, cm^{-1}): 2030s (terminal ν_{N3}). ^{1}H NMR ($CDCl_3$, δ): 1.88 (s, 18H, HMB), 7.41–7.55 (m, 15H, Ph). ^{31}P {^{1}H} NMR ($CDCl_3$, δ): 34.66. Elemental analysis (%) for $C_{30}H_{33}RuN_6P$: Calculated – C, 59.10; H, 5.45; N, 13.78. Found: C, 59.36; H, 5.14; N, 13.92.

2.5.2. Complex **4b**

Yield 36 mg (43%). IR (KBr pellets, cm^{-1}): 2037s (terminal ν_{N3}). ^{1}H NMR ($CDCl_3$, δ): 1.66 (s, 6H, CH_3), 1.89 (s, 18H, HMB), 7.47–7.69 (m, 5H, Ph). ^{31}P {^{1}H} NMR ($CDCl_3$, δ): 29.33. Elemental analysis (%) for $C_{20}H_{29}RuN_6P$: Calculated – C, 49.43; H, 6.02; N, 17.31. Found: C, 49.36; H, 5.86; N, 7.92.

*2.5.3. Complex **4c***

Yield 45 mg (40%). IR (KBr pellets, cm^{-1}): 2027s. ^1H NMR ($CDCl_3$, δ): 1.86 (s, 18H, HMB), 7.31–7.72 (m, 15H, Ph).Elemental analysis (%) for $C_{30}H_{33}RuN_6$ As: Calculated – C, 55.13; H, 5.09; N, 12.85. Found: C, 55.28; H, 5.35; N, 12.45.

*2.6. Synthesis of [(η^6-C_6Me_6)Ru(N_3)$_2$ (L)] {L = Hpz (**5a**), 3-Hmpz (5b), 3,5-Hdmpz (**5c**)}*

A mixture of complex **2** (60 mg, 0.086 mmol) and ligand **L** (0.260 mmol) was stirred in dry acetone (10 ml) for 10 h at room temperature. The solvent was removed under reduced pressure. The solid mass was dissolved in dichloromethane and then filtered. The solution was concentrated for 2 ml and excess of hexane was added for precipitation. The orange yellow product was separated out, washed with diethyl ether and dried under vacuum.

*2.6.1. Complex **5a***

Yield 45 mg (63%). IR (KBr pellets, cm^{-1}): 2037s (terminal ν_{N3}). ^1H NMR ($CDCl_3$, δ): 2.11 (s, 18H, HMB), 6.42 (t, 1H, J = 3.18, CHpz), 7.59 (d, 1H, J = 2.89, CHpz), 7.78 (d, 1H, J = 3.43, CHpz), 11.71 (s, 1H, NH). Elemental analysis (%) for $C_{15}H_{22}RuN_8$: Calculated – C, 43.36; H, 5.33; N, 26.97. Found: C, 43.09; H, 5.62; N, 26.12.

*2.6.2. Complex **5b***

Yield 42 mg (57%). IR (KBr pellets, cm^{-1}): 2037s (terminal ν_{N3}). ^1H NMR ($CDCl_3$, δ): 2.04 (s, 18H, HMB), 2.76 (s, 3H, CH_3), 6.38 (d, 1H, J = 2.66, CHpz), 7.96 (d, 1H, J = 2.92, CHpz), 11.86 (s, 1H, NH). Elemental analysis (%) for $C_{16}H_{24}RuN_8$: Calculated – C, 44.74; H, 5.63; N, 26.08. Found: C, 44.31; H, 5.38; N, 26.17.

*2.6.3. Complex **5c***

Yield 51 mg (67%). IR (KBr pellets, cm^{-1}): 2037s (terminal ν_{N3}). ^1H NMR ($CDCl_3$, δ): 2.05 (s, 18H, HMB), 2.13 (s, 6H, CH_3), 6.45 (s, 1H, CHpz), 11.42 (s, 1H, NH). Elemental analysis (%) for $C_{17}H_{26}RuN_8$: Calculated – C, 46.03; H, 5.91; N, 25.26. Found: C, 46.16; H, 5.73; N, 25.37.

*2.7. Synthesis of [{(η^6-C_6Me_6)Ru(N_3)$_2$}$_2$ (μ-L)] {L = dppm (**6**), dppe (7) and dppp (**8**)}*

A mixture of complex **2** (60 mg, 0.086 mmol) and ligand **L** (0.086 mmol) was stirred in dry acetone (10 ml) for 3 h at room temperature. The solvent was rotary evaporated. The solid was dissolved in dichloromethane and then filtered. The solution was concentrated for 2 ml and excess of hexane was added for precipitation. The orange-yellow product was separated out, washed with hot hexane and diethyl ether, and finally dried under vacuum.

*2.7.1. Complex **6***

Yield 79 mg (85%). IR (KBr pellets, cm^{-1}): 2037s (terminal ν_{N3}). ^1H NMR ($CDCl_3$, δ): 1.82 (s, 36H, HMB), 2.14–2.17 (m, 2H, CH_2), 7.10–7.34 (m, 20H, Ph). ^{31}P {^1H} NMR ($CDCl_3$, δ): 32.62 (s). Elemental analysis (%) for $C_{49}H_{58}Ru_2N_{12}P_2$: Calculated – C, 54.57; H, 5.42; N, 15.58. Found: C, 53.97; H, 5.09; N, 15.35.

2.7.2. Complex 7

Yield 75 mg (80%). IR (KBr pellets, cm^{-1}): 2037s (terminal ν_{N3}). ^1H NMR ($CDCl_3$, δ): 1.75 (s, 36H, HMB), 2.14–2.18 (m, 4H, CH_2), 7.41–7.53 (m, 20H, Ph). ^{31}P {^1H} NMR ($CDCl_3$, δ): 31.13 (s). Elemental analysis (%) for $C_{50}H_{60}Ru_2N_{12}P_2$: Calculated – C, 54.94; H, 5.54; N, 15.38. Found: C, 54.63; H, 5.09; N, 15.42.

*2.7.3. Complex **8***

Yield 81 mg (85%). IR (KBr pellets, cm^{-1}): 2037s (terminal ν_{N3}). ^1H NMR ($CDCl_3$, δ): 1.75 (s, 36H, HMB), 2.14–2.16 (m, 6H, CH_2), 7.27–7.47 (m, 20H, Ph). ^{31}P {^1H} NMR ($CDCl_3$, δ): 28.12 (s). Elemental analysis (%) for $C_{51}H_{62}Ru_2N_{12}P_2$: Calculated – C, 55.36; H, 5.64; N, 15.19. Found: C, 55.52; H, 5.46; N, 15.02.

*2.8. Syntheses of [(η^6-C_6Me_6)Ru(N_3)(Cl)(L)] {L = PPh_3 (**9a**), PMe_2Ph (**9b**), $AsPh_3$ (**9c**)}*

These complexes were synthesized using the same procedure given above (see 2.5), except that complex [(η^6-C_6Me_6)Ru(-N_3)(Cl)]$_2$ **3** (60 mg, 0.088 mmol) was used as the starting material instead of complex **2**.

*2.8.1. Complex **9a***

Yield 41 mg (39%). IR (KBr pellets, cm^{-1}): 2037s (terminal ν_{N3}). ^1H NMR ($CDCl_3$, δ): 1.82 (s, 18H, HMB), 6.94–7.56 (m, 15H, Ph). ^{31}P {^1H} NMR ($CDCl_3$, δ): 33.68. Elemental analysis (%) for $C_{30}H_{33}RuN_3ClP$: Calculated – C, 59.74; H, 5.51; N, 6.96. Found: C, 59.39; H, 5.87; N, 7.06.

*2.8.2. Complex **9b***

Yield 37 mg, (44%). IR (KBr pellets, cm^{-1}): 2037s (terminal ν_{N3}). ^1H NMR ($CDCl_3$, δ): 1.54 (s, 6H, CH_3), 1.76 (s, 18H, HMB), 7.43–7.51 (m, 5H, Ph). ^{31}P {^1H} NMR ($CDCl_3$, δ): 30.43. Elemental analysis (%) for $C_{20}H_{29}RuN_3ClP$: Calculated – C, 50.15; H, 6.10; N, 8.77. Found: C, 49.12; H, 5.86; N, 8.43.

*2.8.3. Complex **9c***

Yield 46 mg, (41%). IR (KBr pellets, cm^{-1}): 2037s (terminal ν_{N3}). ^1H NMR ($CDCl_3$, δ): 1.78 (s, 18H,

HMB), 6.91–7.65 (m, 15H, Ph). Elemental analysis (%) for $C_{30}H_{33}RuN_3ClAs$: Calculated – C, 55.68; H, 5.14; N, 6.49. Found: C, 55.37; H, 4.97; N, 6.62.

2.9. Synthesis of [{(η^6-C_6Me_6)Ru(N_3)Cl}$_2$ (μ-L)] {L = dppm (**10**), dppe (11) and dppp (**12**)}

A mixture of complex **3** (60 mg, 0.086 mmol) and ligand **L** (0.086 mmol) was stirred in dry acetone (10 ml) for 3 h at room temperature. The solvent was rotary evaporated. The solid was dissolved in dichloromethane and then filtered. The solution was concentrated for 2 ml and excess of hexane added for precipitation. The orange-yellow product was separated out, washed with hot hexane and diethyl ether, and finally dried under vacuum.

2.9.1. Complex **10**

Yield 81 mg, (86%). IR (KBr pellets, cm^{-1}): 2037s (terminal ν_{N3}). ^1H NMR ($CDCl_3$, δ): 1.74 (s, 36H, HMB), 2.13–2.15 (m, 2H, CH_2), 7.23–7.42 (m, 20H, Ph). ^{31}P {^1H} NMR ($CDCl_3$, δ): 30.56(s). Elemental analysis (%) for $C_{49}H_{58}Ru_2N_6Cl_2P_2$: Calculated – C, 55.26; H, 5.48; N, 7.89. Found: C, 55.48; H, 5.04; N, 8.01.

2.9.2. Complex **11**

Yield 85 mg, (89%). IR (KBr pellets, cm^{-1}): 2037s (terminal ν_{N3}). ^1H NMR ($CDCl_3$, δ): 1.82 (s, 36H, HMB), 2.13–2.20 (m, 4H, CH_2), 7.38–7.61 (m, 20H, Ph). ^{31}P {1H} NMR ($CDCl_3$, δ): 30.34 (s). Elemental analysis (%) for $C_{50}H_{60}Ru_2N_6Cl_2P_2$: Calculated – C, 55.64; H, 5.60; N, 7.78. Found: C, 55.35; H, 5.41; N, 7.97.

2.9.3. Complex **12**

Yield 82 mg, (85%). IR (KBr pellets, cm^{-1}): 2037s (terminal ν_{N3}). ^1H NMR ($CDCl_3$, δ): 1.74 (s, 36H, HMB), 2.14–2.19 (m, 6H, CH_2), 7.24–7.48 (m, 20H, Ph). ^{31}P {^1H} NMR ($CDCl_3$, δ): 27.46 (s). Elemental analysis (%) for $C_{51}H_{62}Ru_2N_6Cl_2P_2$: Calculated – C, 56.02; H, 5.71; N, 7.68. Found: C, 56.25; H, 5.48; N, 7.52.

2.10. Synthesis of [{(η^6-C_6Me_6)Ru(N_3)Cl}$_2$ (μ-4,4-bipy)] (**13**)

A mixture of complex **3** (60 mg, 0.088 mmol) and 4,4-bipyridine (0.088 mmol) in dry acetone (15 ml) was stirred for 3 h, and the solvent was removed under vacuum. The solid product was washed with diethylether (10 ml × 2) and then dried under vacuum to give the yellow solid complex **13**.

Yield 62 mg, (84%). IR (KBr pellets, cm^{-1}): 2037s (terminal ν_{N3}). ^1H NMR ($CDCl_3$, δ): 2.05 (s, 36H, HMB), 7.55–7.69 (m, 4H), 8.75–8.94 (m, 4H). Elemental analysis (%) for $C_{34}H_{44}Ru_2N_8Cl_2$: Calculated – C, 48.74; H, 5.27; N, 13.37. Found: C, 48.82; H, 5.41; N, 13.53.

3. Structure analysis and refinement

Single crystals of complexes **2**, **3**, **4a** and **6** suitable for X-ray analyses were grown by slow diffusion of diethylether into their solution in a mixture of dichloromethane and acetone. X-ray intensity data were collected on a Rigaku Mercury CCD area detector employing graphite-monochromated Mo Kα radiation (λ = 0.71069 Å) at a temperature of 143 K. Indexing was performed from a series of twelve 0.5° rotation images with exposures of 30 s. Rotation images were processed using crystal clear [14], producing a listing of unaveraged F^2 and σ (F^2) values, which were then passed on to the crystal structure [14] program package for further processing and structure solution on a Dell Pentium III computer. The intensity data were corrected for Lorentz and polarization effects and for absorption using the REQAB program [15].

The structure was solved by direct methods (SIR-97) [16]. Refinement was performed by a full-matrix least-squares method based on F^2 using SHELXL-97 [17]. All reflections were used during refinement (F^2 that were experimentally negative were replaced by $F^2 = 0$). The weighting scheme used was $W = 1/[\sigma^2(F_o^2) + 0.0235P^2 + 1.7407P]$ for the complex **2**, $W = 1/[\sigma^2(F_o^2) + 0.0308P^2 + 2.5803P]$ for complex **4a**, and $W = 1/[\sigma^2(F_o^2) + 0.0559P^2 + 2.6157P]$ for complex **6**, where $P = (F_o^2 + 2F_c^2)/3$. Non-hydrogen atoms were refined anisotropically, while hydrogen atoms were refined using a "riding" model. Refinement converged at a final value of R = 0.0245, 0.0411, 0.0302 and 0.0366 for the complexes **2**, **3**, **4a** and **6**, respectively (for observed data F), and at values of wR_2 = 0.0576, 0.0950, 0.0724 and 0.0957 for complexes **2**, **3**, **4a** and **6**, respectively (for unique data F^2) (see Scheme 1).

Table 1 lists the cell information, data collection parameters and refinement data. Figs. 1–4 are ORTEP [18] representations of complexes **2**, **3**, **4a** and **6** with 30% probability thermal ellipsoids displayed (except complex **3** with 50% probability).

4. Results and discussion

4.1. Dimeric complexes

The chloro arene ruthenium dimer **1** reacted with excess of sodium azide in ethanol gave an orange-colored tetraazido complex **2** in 92% yield. When the reaction was carried out with the complex **1** and sodium azide in 1:2 molar ratios in acetone, the orange-red di-azido complex **3** was obtained in 85% yield. The similar

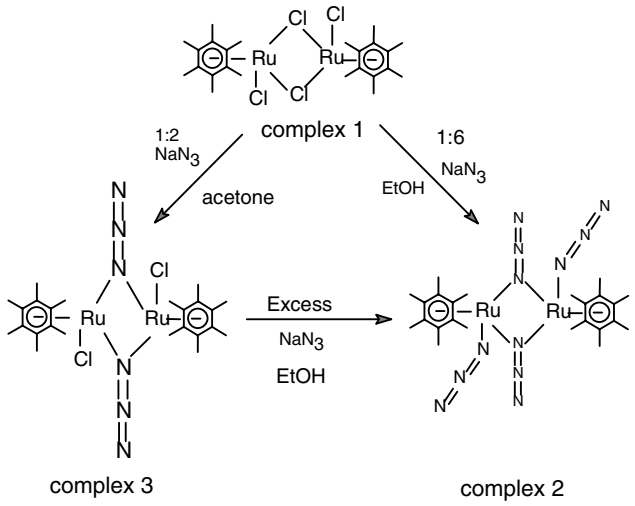

Scheme 1.

reaction in the case of *p*-cymene dimer $[(\eta^6\text{-}C_{10}H_{14})Ru(\mu\text{-}Cl)Cl]_2$ invariably yielded only the bridged disubstituted azido complex $[(\eta^6\text{-}C_{10}H_{14})Ru(\mu\text{-}N_3)Cl]_2$ analogous to complex **3** [19a]. It is very interesting to see the difference of the reactivity of these dimers (**2** and **3**) towards azide as observed in the case pyrazole reactions [12b]. In the case of pyrazole reactions, one can understand the difference of the reactivity of these dimers towards pyrazoles on the basis of steric factor of pyrazoles as well as hexamethylbenzene. The complex **3** with excess of sodium azide gave the complex **2**. These complexes are stable in air and soluble in polar solvents such as chloroform and dichloromethane, but insoluble in non-polar solvents such as hexane and pentane.

The infrared spectrum of complex **2** shows two characteristic stretching bands – one in the region of the terminal azide ligands at 2024 cm^{-1} and another in the region of the bridging azide ligands at 2064 cm^{-1} [20] indicating the complex **2** have two types of azide groups. Where as in the case of complex **3** exhibit the characteristic band for the bridging azide groups at 2057 cm^{-1}, demonstrating that no terminal azide ligands are present. This is further confirmed by the elemental analysis, which indicates only two azide groups. The proton NMR spectrum of the complex **2** exhibits a strong peak at 2.06 ppm for the hexamethylbenzene protons, whereas in the case of complex **3** the signal is observed at 2.09 ppm.

4.2. Mononuclear complexes

The dimeric complexes **2** and **3** undergo bridge cleavage reactions with a twofold excess of ligand **L** in acetone, giving the mononuclear complexes **4**, **5**, and **9** (Scheme 2).

The infrared spectra of complexes **4** and **9** show a strong band in the range of 2037–2026 cm^{-1} due to the terminal azide group [21] along with strong bands due to the phenyl groups of the phosphine ligands.

Table 1
Crystal data and structure refinement for complexes **2**, **3**, **4a** and **6** acetone

Formula	$C_{24}H_{36}N_{12}Ru_2$	$C_{24}H_{36}Cl_2N_6Ru_2$	$C_{30}H_{33}N_6PRu$	$C_{52}H_{64}N_{12}P_2ORu_2$
M_r	694.79	681.63	609.66	1137.23
Wavelength (Å)	0.71069	0.71073	0.71069	0.71069
Crystal system	Monoclinic	Triclinic	Monoclinic	Triclinic
Space group	$P2_1/n$	$P\bar{1}$	$P2_1/c$	$P\bar{1}$
Unit cell dimensions				
a (Å)	8.6152(5)	9.169(2)	18.037(2)	11.5469(5)
b (Å)	16.1555(10)	9.178(2)	8.5409(7)	13.1587(4)
c (Å)	10.4889(7)	9.365(2)	17.9964(13)	18.6027(5)
α (°)	90	111.208(4)	90	69.563(3)
β (°)	110.468(1)	102.294(4)	100.383(2)	83.811(4)
γ (°)	90	106.566(4)	90	78.166(4)
V (Å^3)	1367.7(2)	658.6(3)	2726.9(4)	2590.3(2)
Z	2	1	4	2
Crystal size (mm^3)	$0.35 \times 0.12 \times 0.06$	$0.05 \times 0.04 \times 0.03$	$0.32 \times 0.30 \times 0.04$	$0.32 \times 0.20 \times 0.10$
D_{calc} (g cm$^-$ 3)	1.687	1.718	1.485	1.458
$F(000)$	704	344	1256	1172
2θ (°)	5.04–54.96	4.96–56.36	5.3–54.96	5.36–54.96
Reflections collected	7973	5765	35422	32462
Independent	2971	5155	6111	11506
Reflections [R(int)]	0.0152	0.0164	0.0239	0.0197
μ (Mo Kα)/cm^{-1}	11.43	1.374	6.65	6.95
No. parameters	179	296	350	635
Goodness of-fit on F^2	1.097	0.983	1.0124	1.055
R_1 ($I > 2\sigma(I)$), wR_2	0.0245, 0.0576	0.0411, 0.0950	0.0302, 0.0724	0.0366, 0.0957
R_1, R_2 (all data)	0.0266, 0.0592	0.0523, 0.1006	0.0330, 0.0737	0.0406, 0.0998
Largest diff. peak and hole (e Å^{-3})	+1.152, −0.550	+0.807, −0.403	+0.804, −0.853	+1.691, −1.134

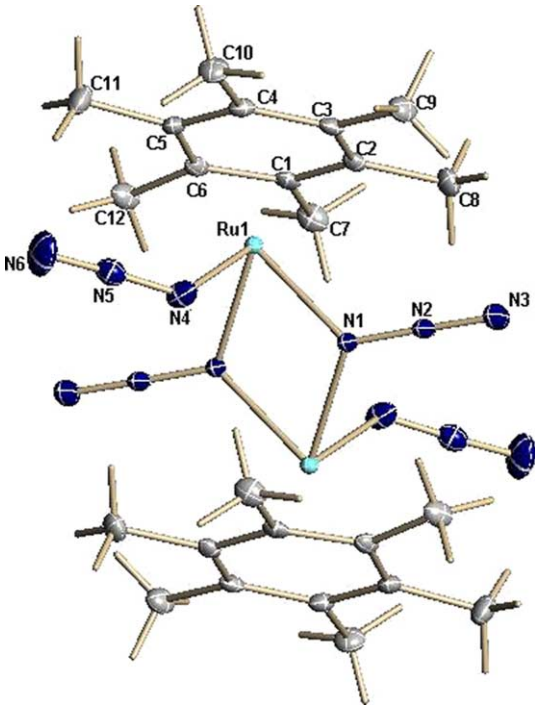

Fig. 1. ORTEP diagram of the complex **2** with 30% probability thermal ellipsoids. Selected bond lengths (Å) and bond angles (°)

Bond lengths (Å)	
Ru(1)–N(1)	2.148(2)
Ru(1)–N(4)	2.141(2)
N(1)–N(2)	1.208(3)
N(2)–N(3)	1.140(3)
N(4)–N(5)	1.084(3)
N(5)–N(6)	1.191(4)
Ru–C*	1.663
Bond angles (°)	
N(4)–Ru(1)–N(1)	84.33(8)
N(1)#(1)–Ru(1)–N(1)	73.26(8)
N(4)–Ru(1)–N(1)#(1)	82.59(9)

* Ruthenium to centroid of HMB.

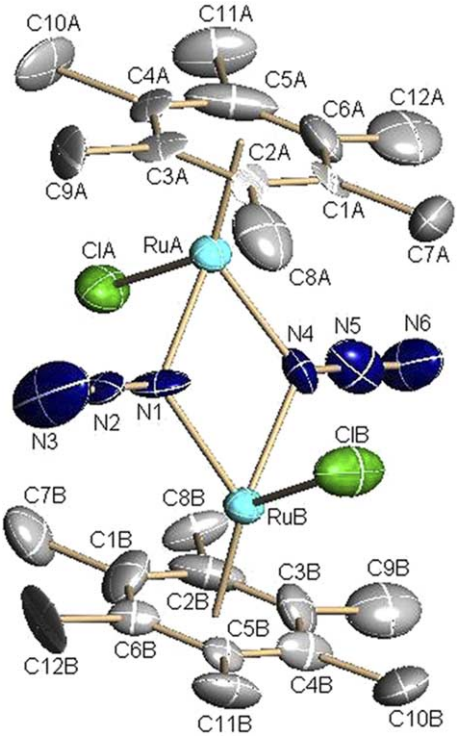

Fig. 2. ORTEP diagram of the complex **3** with 50% probability thermal ellipsoids. Hydrogens are omitted for clarity of the figure. Selected bond lengths (Å) and bond angles (°)

Bond lengths (Å)	
Ru(A)–C*	1.714
Ru(B)–C*	1.614
Ru(A)–Cl(A)	2.394(5)
Ru(A)–N(1)	2.120(14)
Ru(A)–N(4)	2.138(13)
Ru(B)–Cl(B)	2.421(5)
Ru(B)–N(1)	2.151(12)
Ru(B)–N(4)	2.168(14)
N(1)–N(2)	1.189(19)
N(2)–N(3)	1.11(2)
N(4)–N(5)	1.23(2)
N(5)–N(6)	1.17(2)
Bond angles (°)	
N(1)–Ru(A)–Cl(A)	87.4(4)
N(4)–Ru(A)–Cl(A)	87.6(4)
N(1)–Ru(A)–N(4)	71.9(4)
N(1)–Ru(B)–Cl(B)	84.4(4)
N(4)–Ru(B)–Cl(B)	86.5(4)
N(1)–Ru(B)–N(4)	70.7(4)

* Ruthenium to centroid of HMB.

The monomeric compounds exhibit only one IR band due to terminal azide group which is slightly higher wave number with comparison to the starting dimer. The ^{1}H NMR spectra of these complexes exhibit a strong peak for hexamethylbenzene at 1.88 ppm for complex **4a**,1.89 ppm for complex **4b** and 1.86 ppm for complex **4c**, indicating an upfield shift from 2.08 ppm for the HMB protons in the starting complex. This is due to the increased electron density on the ruthenium atom induced by the two azide groups. The aromatic protons of the ligands **L** appear as multiplets at around 6.91–7.69 ppm for these complexes. The ^{31}P $\{^{1}$H$\}$ NMR spectra of these complexes exhibit a singlet at around 29.33–34.66 ppm for the terminal phosphine group. The ^{1}H NMR spectra of the complexes **9a**–**c** also exhibit strong signals for the hexamethylbenzene protons in the range at 1.76–1.89 ppm and multiplets in the range of 7.0–7.7 ppm for the phenyl groups of the phosphine ligands. The methyl protons of PMe_2Ph appear around 1.66 ppm in the case of complex **4b** and around 1.54 ppm in the case of complex **9b**.

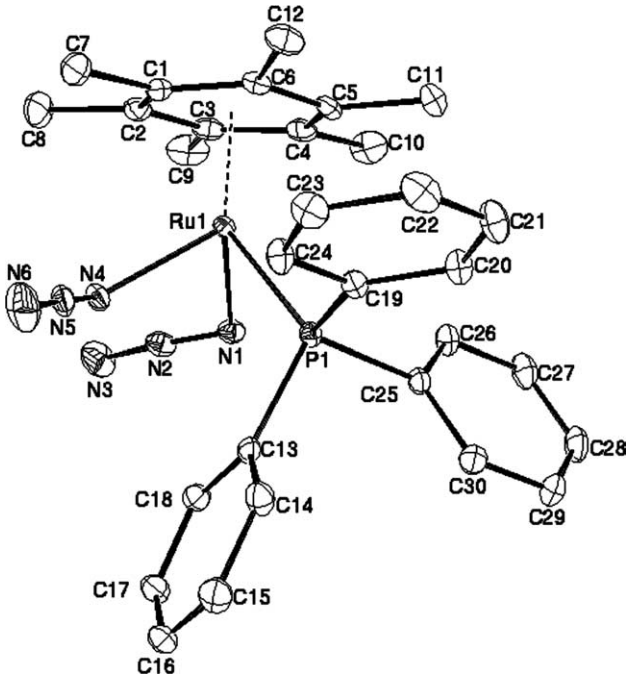

Fig. 3. ORTEP diagram of the complex **4a** with 30% probability thermal ellipsoids. Hydrogens are omitted for clarity of the figure. Selected bond lengths (Å) and bond angles (°)

Bond lengths (Å)	
Ru(1)–N(1)	2.145(2)
Ru(1)–N(4)	2.105(2)
N(1)–N(2)	1.203(3)
N(2)–N(3)	1.203(3)
N(4)–N(5)	1.192(3)
N(5)–N(6)	1.158(3)
Ru(1)–P(1)	2.3604(5)
Ru–C[a]	2.242
Bond angles (°)	
N(4)–Ru(1)–N(1)	84.03(7)
N(4)–Ru(1)–P(1)	87.77(5)
N(1)–Ru(1)–P(1)	86.32(5)

[a] Average distance between ruthenium and HMB.

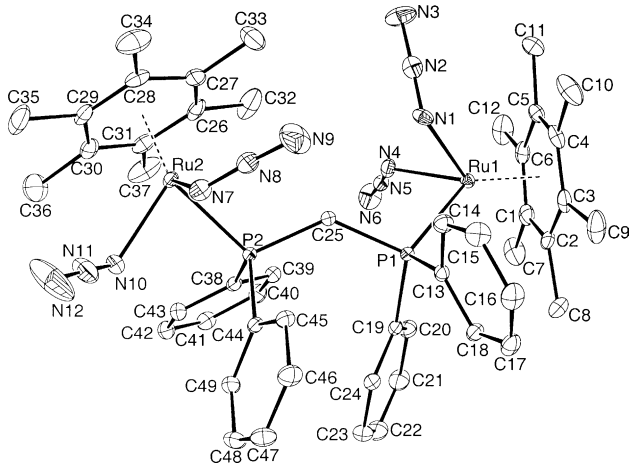

Fig. 4. ORTEP diagram of the complex **6** with 30% probability thermal ellipsoids. Hydrogens are omitted for clarity of the figure. Selected bond lengths (Å) and bond angles (°)

Bond lengths (Å)	
Ru(1)–N(4)	2.145(2)
Ru(1)–N(1)	2.105(2)
Ru(1)–P(1)	2.3756(6)
P(1)–C(25)	1.158(3)
P(2)–C(25)	1.836(2)
Ru(2)–N(10)	2.127(2)
Ru(1)–C*	2.238
Ru(2)–N(7)	2.089(2)
Ru(2)–P(2)	2.3594(6)
Ru(2)–C*	2.233
Bond angles (°)	
N(4)–Ru(1)–N(1)	83.09(9)
N(4)–Ru(1)–P(1)	84.95(6)
N(1)–Ru(1)–P(1)	81.18(6)
N(7)–Ru(2)–N(10)	83.56(9)
N(7)–Ru(2)–P(2)	86.80(6)
N(10)–Ru(2)–P(2)	82.21(6)

* Average distance between ruthenium and HMB.

The IR spectrum of complex **5** shows a strong band at 2037 cm^{-1} due to the terminal azide mode of the complex which is higher wave number comparatively to starting complex. Peak integration of the ^1H NMR spectrum of complex **5** shows these complexes are mononuclear in nature. The methyl protons of hexamethylbenzene appear as a strong singlet at around 2.04–2.11 ppm. The NH proton of the pyrazole ligands shifts downfield and appears at around 11.5 ppm [12b]. The ring CH protons of pyrazoles appear in the aromatic region.

4.3. Binuclear bridging complexes

The reaction of the complex **2** and **3** with bridging phosphine ligands in acetone resulted in the formation of orange colored, air-stable binuclear complexes **6–8** and **10–12** (Scheme 3). The formation of these complexes is confirmed by the ^1H NMR spectra. The IR spectra of these complexes show the terminally bound azide ligands at 2037 cm^{-1} [21] along with strong bands due to the phenyl groups of the phosphine ligands.

The aromatic protons of the ligand **L** appear as multiplets at around 7.10–7.61 ppm for these complexes. The multiplets in the range 2.13–2.20 ppm are assigned to the methylene groups of the phosphine ligands. The ^{31}P $\{^1H\}$ NMR spectra of these complexes exhibit a singlet at around 27.46–32.62 ppm for the bridged phosphine group indicating the symmetric nature of the complexes.

The reaction of the complex **3** with 4, 4′-bipyridine ligand in acetone resulted in the formation of the orange

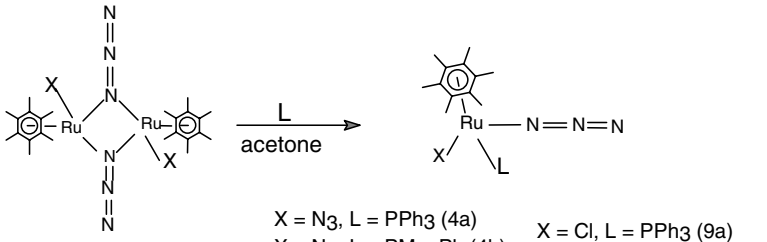

Scheme 2.

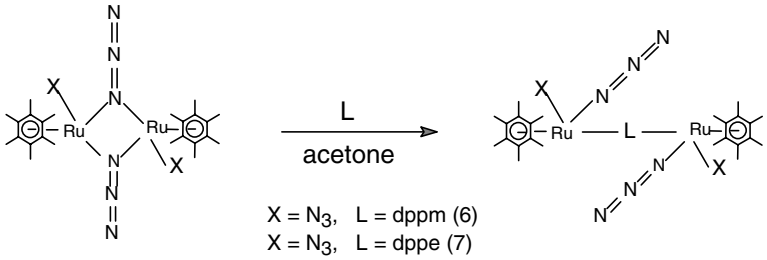

Scheme 3.

colored binuclear complex **13** (Scheme 3). The infrared spectrum of complex **13** shows a strong band at 2037 cm^{-1} due to the terminal azide group. The ^1H NMR spectrum of complex **13** exhibits a strong singlet for hexamethyl-benzene protons at 2.05 ppm. The ligand bipy protons are observed as four doublets in the region 7.55–8.94 ppm.

5. Molecular structures

Single crystals of the complexes **2**, **3**, **4a** and **6** were subject to X-ray crystal studies. A summary of the single-crystal X-ray structure analyses is shown in Table 1. The ORTEP drawings of the complexes **2**, **3**, **4a** and **6** are shown in Figs. 1–4, respectively. The geometry around the ruthenium atom in these complexes **2**, **3**, **4a** and **6** is octahedral, where the hexamethylbenzene ligand occupies three coordination positions.

The complex $[\{(\eta^6\text{-}C_6Me_6)Ru(\mu\text{-}N_3)(N_3)\}_2]$ **2** crystallizes in the monoclinic space group $P_2(1)/n$ with centrosymmetry. The compound has a structure describable as the joining of two piano stools together by their legs. The bond angle N(1)–Ru(1)–N(4) around ruthenium equals 84.33(8)°, a little lower than that for other reported compounds. The bond distance between the centroid of HMB and Ru is 1.663 Å, while the Ru–N bond distances are 2.148(2) Å for the Ru(1)–N(1) bond and 2.141(2) Å for the Ru(1)–N(4) bond, which are within the limits observed for reported complexes [22]. The terminal azide nitrogens have N–N bond distances of 1.084(3) Å for the (N4)–(N5) bond and 1.191(3) Å for the (N5)–(N6) bond. The N–N bond distances in the bridging azide nitrogens are 1.208(3) Å for the (N1)–(N2) bond and 1.140(3) Å for the (N2)–(N3) bond. In the case of terminal azide, the N(4)–N(5) bond distance is slightly smaller than the bridging azide N(1)–N(2), whereas the N(5)–N(6) distance of the terminal azide is slightly longer than the bridging azide N(2)–N(3) distances. However, these bond distances for the bridging and terminal azide N–N bonds are close to other reported values [19].

The complex $[\{(\eta^6\text{-}C_6Me_6)Ru(\mu\text{-}N_3)Cl\}_2]$**3** crystallizes in the triclinic space group $P\bar{1}$. It consists of each Ru(II) atom bonded to a hexamethylbenzene ligand, two nitrogen atoms of azide groups and one chlorine atom, maintaining centrosymmetry. The Ru–Cl bond distances are 2.394(5) and 2.421(5) Å, which are close

to those in the starting dimeric complex **1** [23]. The Ru–N bond lengths involving the bridging nitrogen moieties Ru(A)–N(1), Ru(A)–N(4), Ru(B)–N(1) and Ru(B)–N(4) are 2.120(14), 2.138(13), 2.151(12) and 2.168(14) Å, respectively, very similar to those found in the complex **2**. This structure gives N–N bond distances of 1.189(19), 1.11(2), 1.23(2) and 1.17(2) Å, which are slightly shorter than in the complex **2**. The geometry of the complex is octahedral with the hexamethylbenzene ligand occupying three coordination sites. This is evident from the nearly 90° values for the N–Ru–Cl bond angles, which are 87.4(4)° for the N(1)–Ru(A)–Cl(A) angle and 87.6(4)° for the N(4)–Ru(A)–Cl(A) angle. The average distance between ruthenium and the hexamethylbenzene carbons is 2.207 Å for the Ru(A)–C(arene) bonds and 2.128 Å for the Ru(B)–C(arene) bonds. The distances between the centroid of the arene and the metal atoms are 1.714 and 1.614 Å for Ru(A)–C(arene) and Ru(B)–C(arene), respectively.

The structure of the complex $[(\eta^6\text{-}C_6Me_6)Ru(N_3)_2(PPh_3)]$ **4a** consists of a Ru (II) atom η^6-coordinated to a hexamethylbenzene molecule, to the two nitrogen atoms of the azide group, and to a PPh_3 ligand through the P atom, leading to a 'three-legged piano stool' type of structure. The two Ru–N distances (2.105(2) and 2.145(2) Å) are slightly different, as found in related structures with phosphine complexes (2.177(2) Å) [24]. The average Ru–C(arene) distance is 2.242 Å. The arene ring is nearly planar and shows C–C bond distances that appear to be normal. The N(4)–Ru(1)–N(1) bond angle of 84.05(7)° is similar to that found in the related rhodium(III) azido complex $[Rh_2(C_5Me_5)_2(N_3C_4F_6)_3(N_3)]$ (82.0(3)°) [19b]. The N(1)–Ru(1)–P(1) and N(4)–Ru(1)–P(1) bond angles (86.32(5) and 87.77(5)°, respectively) also indicate a piano stool type of structure.

The complex **6** crystallized with one molecule of acetone for each complex molecule. The geometry around each ruthenium center of **6** is close to octahedral, with the hexamethylbenzene ligand occupying three coordination sites. The complex crystallizes in the triclinic space group $P\bar{1}$. as shown in figure **4**. The ruthenium atom is -bonded to the hexamethylbenzene ligand with the average distance between ruthenium and the six membered hexamethylbenzene ring equal to 2.238 Å, thus falling within the range found in other hexamethylbenzene ruthenium complexes [12b]. The Ru-P bond distances of 2.3756(6) and 2.3594(6) Å are similar to those in the mononuclear complex **4a**. The bond angles N(4)–Ru(1)–P(1), N(4)–Ru(1)–N(1), N(7)–Ru2–P(2) and N(7)–Ru(2)–N(10) are 84.95(6), 83.09(9), 86.80(6) and 83.56(9)°, respectively, indicating a piano stool type of structure at each ruthenium center. The dppm moiety acts as a bridging ligand between the two ruthenium centers in this complex.

6. Concluding remarks

It is thus interesting to note that there is a difference in reactivity between the *p*-cymene dimeric complex $[(\eta^6\text{-}p\text{-cymene})Ru(\mu\text{-}Cl)Cl]_2$ and the hexamethylbenzene dimeric complex $[(\eta^6\text{-}C_6Me_6)Ru(\mu\text{-}Cl)Cl]_2$ towards azides and pyrazoles [3b]. The former gives only the disubstituted *p*-cymene ruthenium μ-azido dimer $[(\eta^6\text{-}C_{10}H_{14})Ru(\mu\text{-}N_3)Cl]_2$ irrespective of sodium azide concentration [19a], whereas the latter gives both disubstituted μ-azido and tetrazido substituted complexes. These complexes can undergo a variety of substitution reactions with monodentate and bidentate ligands to yield monomeric compounds as well as bridged dimeric compounds. Complex **3** gives chiral complexes after substitution of neutral ligands. These complexes are very good starting materials for the synthesis of new azido compounds.

Acknowledgement

We thank Professor R.H. Duncan Lyngdoh for his help in preparing the manuscript.

Appendix A. Supplementary material

Crystallographic data for the structural analysis have been deposited at the Cambridge Crystallographic Data Centre (CCDC), CCDC No. **235560** for complex **2**, CCDC No. **247740** for complex **3**, CCDC No. **247738** for complex **4a**, and CCDC No. **247739** for complex **6**. Copies of this information may be obtained free of charge from the director, CCDC, 12 Union Road, Cambridge, CB2 1EZ, UK (fax: +44-1223-336033; e-mail: deposit@ccdc.cam.ac.uk or www: http://www.ccdc.cam.ac.uk). Supplementary data associated with this article can be found, in the online version at doi:10.1016/j.jorganchem.2004.10.039.

References

[1] C.S. Slone, D.A. Weinberger, C.A. Mirkin, Prog. Inorg. Chem. 48 (1999) 233.
[2] (a) P. Jutzi, M.O. Kristen, B. Neumann, H.-G. Stammler, Organometallics 13 (1994) 3584;
(b) A. Baretta, K.S. Chong, F. Geoffrey, N. Cloke, A. Feigenbaum, M.L.H. Green, J. Chem. Soc., Dalton Trans. (1983) 861;
(c) P. Julzi, T. Redeker, Eur. J. Inorg. Chem. (1998) 663;
(d) M.S. Blais, J.C.W. Chien, M.D. Rausch, Organometallics 17 (1998) 3775;
(e) P. Jutzi, M.O. Kristen, J. Dahlhaus, B. Neumann, H.–G. Stammler, Organometallics 12 (1993) 2980;
(f) D.B. Grotjahn, C. Joubran, D. Combs, D.C. Brune, J. Am. Chem. Soc. 120 (1998) 11814;
(g) T.–F. Wang, C.–C. Hwu, C.–W. Tsai, Y.–S. Wen, Organometallics 17 (1998) 131;

(h) T.–F. Wang, C.–C. Hwu, C.W. Tsai, Y.S. Wen, J. Chem. Soc., Dalton Trans. (1998) 2901.
[3] (a) S.D.R. Christie, K.W. Man, R.J. Whitby, A.M.Z. Slawin, Organometallics 18 (1999) 348;
(b) D. Deng, C. Oian, G. Wu, P. Zheng, J. Chem. Soc., Chem Commun. (1990) 880;
(c) A.A.H. Vander Zeijden, C. Mattheis, R. Frahlich, Organometallics 16 (1997) 2651;
(d) A.A.H. Vander Zeijden, C. Mattheis, R. Frahlich, F. Zippel, Inorg. Chem. 36 (1997) 4444.
[4] (a) I. Lee, F. Dahan, A. Maisonnat, R. Poilblane, Organometallics 13 (1994) 2743;
(b) L. Lefort, T.W. Crane, M.D. Farwell, D.M. Baruch, J.A. Kaeuper, R.J. Lachicotte, W.D. Jones, Organometallics 17 (1998) 3889;
(c) L.P. Barthel–Rosa, V.J. Catalono, K. Maitra, J.H. Nelson, Organometallics 15 (1996) 3924.
[5] (a) S.G. Davies, J.P. McNally, A.J. Smallridge, Adv. Organomet. Chem. 30 (1991) 1 (and references therein);
(b) M.A. Bennett, K. Khan, E. Wenger, Comprehensive Organometallic Chemistry, Elsevier, Oxford, 1995 (and references therein);
(c) B.M. Trost, J.A. Marting, R.J. Kulawiec, A.F. Indoles, J. Am. Chem. Soc. 115 (1993) 10402;
(d) P. Pertici, V. Ballantini, P. Salvadori, M.A. Bennett, Organometallics 14 (1995) 2565;
(e) M.A. Harerov, F. Urberos, B. Chadred, Organometallics 12 (1993) 95.
[6] C.S. Allardyce, P.J. Dyson, D.J. Ellis, P.A. Salter, R. Scopelliti, J. Organomet. Chem. 668 (2003) 35.
[7] H. Harvath, G. Laurency, A. Katho, J. Organomet. Chem. 689 (2004) 1036.
[8] I.W. McNae, K. Fishburne, A. Habtemariam, T.M. Hunter, M. Melchart, F. Wang, M.D. Walkinshaw, P.J. Sadler, J. Chem. Soc., Chem. Commun. (2004) 1786.
[9] W.S. Han, S.W. Lee, J. Chem. Soc., Dalton Trans. (2004) 1656.
[10] Chao-Wan Chang, Gene-Hsiang Lee, Organometallics 22 (2003) 3107.
[11] P. Govindaswamy, H.P. Yennawar, M.R. Kollipara, J. Organomet. Chem. 689 (2004) 3108.
[12] (a) P. Govindaswamy, Y.A. Mozharivskyj, M.R. Kollipara, Polyhedron (in press);
(b) P. Govindaswamy, Y.A. Mozharivskyj, M.R. Kollipara, J. Organomet. Chem. 689 (2004) 3265.
[13] (a) M.A. Bennett, T.N. Huang, T.W. Matheson, A.K. Smith, Inorg. Synth. 21 (1982) 74;
(b) M.A. Bennett, T.W. Matheson, G.B. Robertson, A.K. Smith, P.A. Tucker, Inorg. Chem. 19 (1980) 1014.
[14] Crystal Structure: Crystal Structure Analysis Package, Rigaku Corp. Rigaku/MSC (2002).
[15] REQAB4: R.A. Jacobsen, (1994). Private Communication.
[16] SIR-97: A. Altomare, M. Burla, M. Camalli, G. Cascarano, C. Giacovazzo, A. Guagliardi, A. Moliterni, G. Polidori, R. Spagna, J. Appl. Cryst. 32 (1999) 115.
[17] SHELXL-97: Program for the Refinement of Crystal Structures, Sheldrick, G.M. (1997), University of Göttingen, Germany.
[18] ORTEP-II: A Fortran Thermal Ellipsoid Plot Program for Crystal Structure Illustrations. C.K. Johnson (1976) ORNL-5138.
[19] (a) R.S. Bates, M.J. Begley, A.H. Wright, Polyhedron 9 (1990) 1113;
(b) W. Rigby, P.M. Bailey, J.A. McCleverty, P.M. Maitlis, J. Chem. Soc., Dalton Trans. (1979) 371.
[20] P. Paul, K. Nag, Inorg. Chem. 26 (1987) 2969.
[21] (a) R.Y.C. Shin, M.A. Bennett, L.Y. Goh, W. Chen, D.C.R. Hockless, W.K. Leong, K. Mashima, A.C. Willis, Inorg. Chem. 42 (2003) 96;
(b) X.L. Lu, J.J. Vittal, E.R.T. Tiekink, G.K. Tan, S.L. Kuan, L.Y. Goh, T.S.A. Hor, J. Organomet. Chem. 689 (2004) 1978.
[22] T.J. Geldbach, D. Drago, P.S. Pregosin, J. Organomet. Chem. 643–644 (2002) 214.
[23] F.B. McCormick, W.B. Gleason, Acta Cryst. C 44 (1998) 603.
[24] P. Pinto, G. Marconi, F.N. Heinemann, U. Zenneck, Organometallics 23 (2004) 374.